Cutting Graphene

DOI: 10.1002/anie.201105920

Strain-Induced Orientation-Selective Cutting of Graphene into Graphene Nanoribbons on Oxidation**

Liang Ma, Jinlan Wang, and Feng Ding**

Laterally confined, thin, and long strips of graphene, that is, graphene nanoribbons (GNRs), are of particular importance in graphene-based electronics and spintronics applications.[1] Great efforts have been devoted to the production of high-quality GNRs by various methods: 1) electron-beam lithography and plasma etching of graphene;[2,3] 2) chemical synthesis;[4–6] 3) sonochemical cutting and electrochemical etching of graphene sheets;[7,8] 4) metal nanoparticle catalyzed unzipping of graphene;[9,10] 5) chemical vapor deposition;[11–13] and 6) unzipping of carbon nanotubes.[14–16] Among these methods, cutting of large-area graphene is the most used technology for GNR fabrication. Chemical oxidation has been widely exploited to synthesize nanometer-sized graphene[17–19] because of preferred alignment of oxygen atoms along the three zigzag directions of graphene hexagonal lattice in the form of epoxy chains.[20,21]

However, due to the high symmetry of the honeycomb lattice of graphene, the directions of epoxy chains formed on graphene sheet are out of control, and thus oxygen cutting leads to formation of graphene quantum dots[17–20,22] (Figure 1 a→b→c→d). Here we propose using uniaxial tensile strain to break the symmetry in the orientation-selective cutting of graphene (Figure 1 a→e→f→g). Our ab initio calculations show that epoxy chains tend to be aligned along a zigzag direction which is nearly perpendicular to the strain. Moreover, the external strain significantly lowers both the reaction barrier and the enthalpy of reaction of graphene cutting along that direction. Hence, GNRs with large and controllable aspect ratios can be synthesized by oxygen cutting of strained graphene.

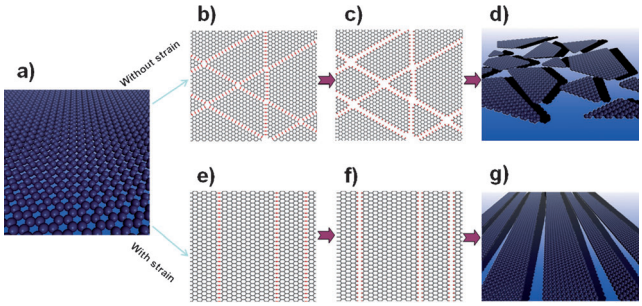

Figure 1. a) Perfect graphene sheet. b)→c)→d) Random cutting of graphene into quantum dots by oxygen attack. e)→f)→g) Orientation-selective cutting of strained graphene into GNRs by oxygen attack.

The calculations were carried out with the Vienna ab initio simulation package (VASP).[23,24] The general gradient approximation (GGA) parameterized by Perdew, Burke, and Ernzerhof (PBE)[25] was used as the exchange-correlation functional, and the projected augmented wave (PAW) method[26,27] was employed to describe the ions–electron interaction. The climbing-image nudged elastic band (CNEB) method[28] incorporated with spin-polarized DFT was used to find the minimum-energy path and locate possible transition states.

In this study, external strain is used to break the symmetry of the graphene honeycomb lattice. The strain was applied along two directions: armchair (AM) and zigzag (ZZ). For strain along the AM direction, the angle between an epoxy chain and the strain θ can be 90 or 30°. For strain along the ZZ direction, θ can be 60 or 0° (Figure 2). For $\theta = 90°$ and $\theta = 0°$, the calculated unit cell contains 32 C and 4 O atoms. For $\theta = 30°$ and $\theta = 60°$, a larger unit cell containing 64 C and 8 O atoms was adopted in the calculation (see Supporting Information, Figure S1). The computational details are elaborated in the Supporting Information.

Clearly, under uniaxial strain, a C–C bond whose orientation is closer to the strain direction is highly elongated and thus more active than others. As a consequence, an epoxy chain with larger θ should be energetically more favorable. To verify the hypothesis, the binding energy (BE) of epoxy chains with $\theta = 90$, 60, 30, and 0° under different strains (0–6%) were calculated. The BE is defined as Equation (1)

$$\mathrm{BE} = [E_{\mathrm{G}}(x) + N_{\mathrm{O}}\,E_{\mathrm{O}} - E_{\mathrm{G-O}}(x)]/N_{\mathrm{O}} \qquad x = 0,\ 1,\ 2,\ 3,\ 4,\ 5,\ 6\,\% \tag{1}$$

where $E_{\mathrm{G-O}}(x)$ and $E_{\mathrm{G}}(x)$ are the energy of graphene with oxygen (G–O) and perfect graphene under x strain, respec-

[*] L. Ma, Prof. J. Wang
Department of Physics & School of Chemistry and Chemical Engineering, Southeast University
Nanjing, 211189 (China)
E-mail: jlwang@seu.edu.cn
Dr. F. Ding
Institute of Textiles and Clothing
Hong Kong Polytechnic University, Kowloon (China)
E-mail: tcfding@inet.polyu.edu.hk

[**] The work at SEU was supported by the NBRP (2010CB923401, 2011CB302004, 2009CB623200), NSF (21173040, 11074035, 20873019), SRFDP (20090092110025), an Outstanding Young Faculty Grant, and the Peiyu Foundation of SEU in China. The work at PolyU was supported by the PolyU research fund (1-ZV3B; A-PD1U; A-PH93; A-PJ50). We thank the computational resource at Department of Physics of SEU and National Supercomputing Center in Tianjin.

Supporting information for this article is available on the WWW under http://dx.doi.org/10.1002/anie.201105920.

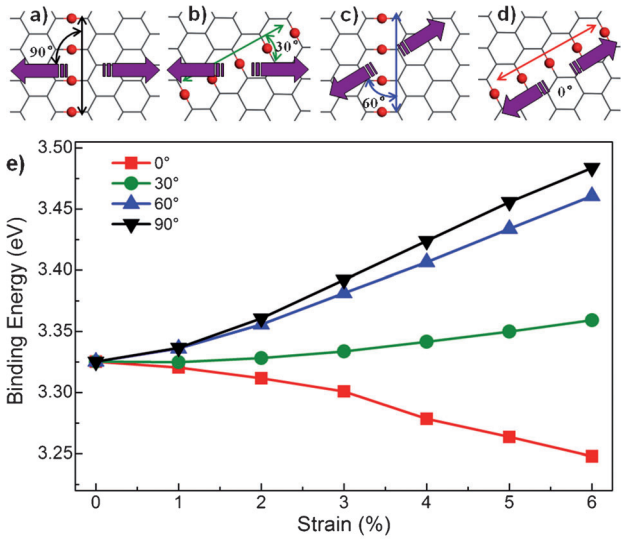

Figure 2. Strain along AM direction: epoxy chains have angles of $\theta = 90°$ (a) and $\theta = 30°$ (b) to the strain. Strain along ZZ direction: epoxy chains have angles of $\theta = 60°$ (c) and $\theta = 0°$ (d) to the strain. e) Binding energies versus strain for $\theta = 0$, 30, 60, and 90° epoxy chains.

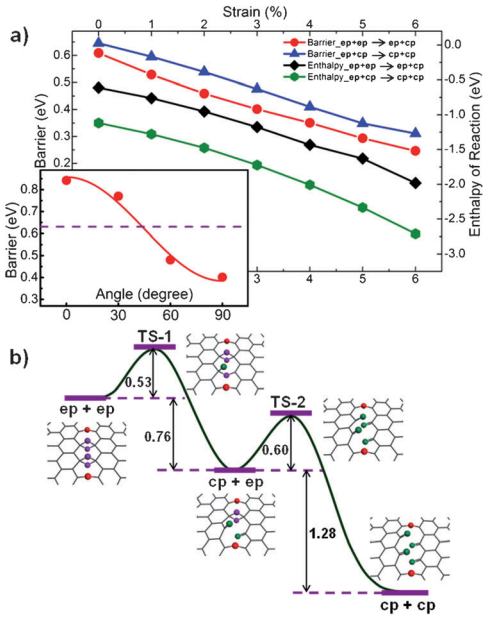

Figure 3. a) Reaction barriers and enthalpies of reaction of the first and second graphene cutting steps. b) Minimum reaction path of two-step graphene cutting with strain $x = 1\%$. The O atoms of epoxy pair(s), unpaired epoxy groups, and carbonyl pair(s) are highlighted as purple, red, and green ball(s), respectively. The inset in a) shows the reaction barriers of **ep** + **ep** → **ep** + **cp** for $\theta = 0$, 30, 60, and 90° epoxy chains preloaded at a strain of $x = 3\%$. The purple dashed line denotes the reaction barrier at a strain of 0%.

tively, E_O is the energy of a free O atom, and N_O is the number of O atoms in the unit cell. As expected: 1) With external strain, the 90° epoxy chain has the highest BE and the 0° one the lowest. 2) Under any external strain, the BE increases monotonically with increasing θ. 3) The BE difference between each two epoxy chains increases monotonically with increasing strain, that is, the higher the strain, the more preferred the alignment the epoxy groups. Although the BE difference of about 0.1–0.2 eV at $x = 2$–5% is not very high, it is enough to significantly bias the O alignment, since the thermal factor $\exp(\Delta E/kT)$ may reach 10^2–10^3 at a reasonable cutting temperature (e.g., $T \approx 300$ K, as the barrier of cutting is lower than 0.7 eV; see Figure 3). Furthermore, the alignment of longer O chains can be more pronounced because of their large formation energy. These results establish that there is an energetically preferred orientation for the epoxy chains on graphene if an external uniaxial strain is applied. Thus, parallel epoxy chains are expected under external strain.

We now consider the cutting of graphene sheet into GNRs under strain. As suggested previously,[21] the selective reaction path of G–O cutting is that an epoxy pair (**ep**) is turned into a carbonyl pair (**cp**) by further oxygen attack. Here we take strained G–O with parallel epoxy chains as reactant. To find the energetically most preferred adsorption site of an additional O atom on G–O, different C–C bridge sites were considered. We found that the opposite side of a preexisting epoxy group is the most active position for a new O atom to form an epoxy pair (Supporting Information, Figure S2).

Next, two possible cutting processes, **ep** → **cp** and **ep** + **ep** → **ep** + **cp**, were calculated for strained G–O with 90° parallel epoxy chains, as it is the energetically most preferred one. Reaction-path analysis revealed that **ep** + **ep** → **ep** + **cp** cutting is energetically more favorable than **ep** → **cp** cutting by 0.1–0.2 eV (Supporting Information, Figure S3). This indicates that an **ep** with another neighboring **ep** breaks into a **cp** more easily than a single **ep**. We thus expect that G–O with preloaded epoxy chains would capture O atoms and form long epoxy-pair chains before breaking into carbonyl-pair chains.

Two-step cutting of G–O (**ep** + **ep** → **ep** + **cp** → **cp** + **cp**) with varying strain ($x = 0$–6%) was also studied. As shown in Figure 3 and Figure S4 of the Supporting Information, increasing the strain from 0 to 6% decreases the reaction barrier of the first/second-step cutting (**ep** + **ep** → **ep** + **cp**/**ep** + **cp** → **cp** + **cp**) remarkably, from 0.61/0.65 eV (strain = 0%) to 0.25/0.31 eV (strain = 6%). Moreover, the differences in enthalpies of reaction (product relative to reactant) are also significant, from −0.61 eV (strain = 0%) to −1.98 eV (strain = 6%) for **ep** + **ep** → **ep** + **cp** and from −1.12 eV (strain = 0%) to −2.71 eV (strain = 6%) for **ep** + **cp** → **cp** + **cp**. The large differences in enthalpies of reaction are mainly due to the release of strain energy. Moreover, the enthalpies of reaction of second-step cutting are much larger than those of first-step cutting, that is, more and more strain energy will be released in further cutting of G–O.

The **ep** → **cp** cutting of G–O with $\theta = 60°$ epoxy chains was also investigated. Similarly, the presence of strain reduces the reaction barriers by 0.42–0.66 eV for first-step cutting (Supporting Information, Figure S5), which again validates our proposed method. In contrast, for $\theta = 0$ or 30°, cutting of strained graphene is more difficult than that of free graphene. As displayed in the inset of Figure 3, the reaction barrier for first-step cutting (**ep** + **ep** → **ep** + **cp**) drops markedly to 0.48/0.40 eV for $\theta = 60/90°$, whereas it increases to 0.84/0.77 eV for

$\theta = 0/30°$ at a strain of $x = 3\,\%$. The change in reaction barrier as a function of strain can be well fitted as Equation (2)

$$E = E_0 + E_1{}^* \cos 2\theta \quad (2)$$

where $E_0 = 0.621$ eV is the reaction barrier at zero strain and $E_1 = 0.236$ eV is a constant. The dependence of reaction energy on angle can be understood in terms of the strain energy released during cutting. As seen in Figure 2, the cutting of G–O releases the stored elastic energy, and the larger the θ, the faster the energy release. Thus, along a large θ, the enthalpy of the reaction becomes smaller due to fast relaxation of the strain. As a consequence, the reaction barrier is also reduced according to the established Bell–Evans–Polanyi principle.[29,30] Although low reaction barriers are demonstrated under tensile strain, it does not mean that the reaction will be out of control. Theoretically, the reaction rate is quantitatively described as $R = CK$, where C is the concentration of the reactant, and $K = 10^{12}\exp(-E_b/kT)$ (E_b: reaction barrier) is the reaction constant. Hence, the reaction can be easily controlled by means of either C or T: slow O supply can be used to reduce the concentration of reactant, and a low temperature can lower the reaction constant.

As the strain in freestanding graphene will be fully released on cutting, we propose a potential experimental route to apply external tensile strain to cut graphene into GNRs (Figure 4):

1) Transfer graphene onto a flexible polymer film and build reasonable binding between graphene and polymer film (e.g., by using glue, Scotch tape, or even the intrinsic ultrastrong adhesion between graphene and substrate[31]).
2) Bend or stretch the polymer film to exert strain on the graphene.
3) Driven by the difference in alignment energy, adsorbed O atoms on the graphene will form parallel epoxy chains.
4) Further oxidation unzips the supported graphene layer into GNRs on the polymer.

As key steps 1) and 2) are both are matured,[32–37] and nanosized graphene has been produced by cutting of preoxidized graphene sheet by a scanning probe microscopic manipulation method,[19] such a cutting procedure should be easily achieved experimentally. Besides, both stretching of graphene on polymer film[32] and oxidation cutting of graphene[19] can be applied to both single- and few-layer graphene.

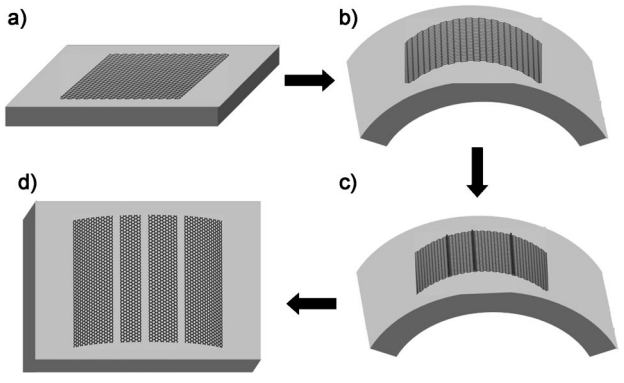

Figure 4. a) Graphene monolayer transferred to a flexible polymer substrate. b) The polymer substrate is bent and thus strain is exerted on the attached graphene sheet. c) Annealing of adsorbed O atoms forms parallel epoxy chains on the graphene. d) Under further oxidation, the graphene layer is unzipped into nanoribbons.

In summary, by using ab initio calculations, we have demonstrated that graphene can be cut into graphene nanoribbons on oxidation with the assistance of a uniaxial external tensile strain. The applied strain plays a crucial role in four respects: 1) It breaks the high symmetry of graphene honeycomb lattice and aligns O atoms along a zigzag direction which is nearly perpendicular to the strain. 2) The presence of the strain remarkably lowers the reaction barriers of graphene cutting along a specific direction. 3) The strain significantly reduces the enthalpies of reaction of graphene cutting along that direction. 4) The strain simultaneously increases the reaction barriers of graphene cutting along other directions. Hence, GNRs with large and controllable aspect ratios are expected to be formed by oxygen cutting of strained graphene.

Received: August 22, 2011
Revised: October 18, 2011
Published online: December 23, 2011

Keywords: ab initio calculations · graphene · nanostructures · nanotechnology

[1] A. H. Castro Neto, F. Guinea, N. M. R. Peres, K. S. Novoselov, A. K. Geim, *Rev. Mod. Phys.* **2009**, *81*, 109.
[2] M. Y. Han, B. Ozyilmaz, Y. B. Zhang, P. Kim, *Phys. Rev. Lett.* **2007**, *98*, 206805.
[3] Z. H. Chen, Y.-M. Lin, M. J. Rooks, P. Avouris, *Physica E* **2007**, *40*, 228.
[4] X. L. Li, X. R. Wang, L. Zhang, S. W. Lee, H. J. Dai, *Science* **2008**, *319*, 1229.
[5] X. Y. Yang, X. Dou, A. Rouhanipour, L. J. Zhi, H. J. Rader, K. Mullen, *J. Am. Chem. Soc.* **2008**, *130*, 4216.
[6] J. M. Cai, P. Ruffieux, R. Jaafar, M. Bieri, T. Braun, S. Blankenburg, M. Muoth, A. P. Seitsonen, M. Saleh, X. L. Feng, K. Mullen, R. Fasel, *Nature* **2010**, *466*, 470.
[7] Z. S. Wu, W. C. Ren, L. B. Gao, B. L. Liu, J. P. Zhao, H.-M. Cheng, *Nano Res.* **2010**, *3*, 16.
[8] L. Tapasztó, G. Dobrik, P. Lambin, L. P. Biro, *Nat. Nanotechnol.* **2008**, *3*, 397.
[9] L. J. Ci, Z. P. Xu, L. L. Wang, W. Gao, F. Ding, K. F. Kelly, B. I. Yakobson, P. M. Ajayan, *Nano Res.* **2008**, *1*, 116.
[10] S. S. Datta, D. R. Strachan, S. M. Khamis, A. T. C. Johnson, *Nano Lett.* **2008**, *8*, 1912.
[11] J. Campos-Delgado, J. M. Romo-Herrera, X. T. Jia, D. A. Cullen, H. Muramatsu, Y. A. Kim, T. Hayashi, Z. F. Ren, D. J. Smith, Y. Okuno, T. Ohba, H. Kanoh, K. Kaneko, M. Endo, H. Terrones, M. S. Dresselhaus, M. Terrones, *Nano Lett.* **2008**, *8*, 2773.
[12] D. C. Wei, Y. Q. Liu, H. L. Zhang, L. P. Huang, B. Wu, J. Y. Chen, G. Yu, *J. Am. Chem. Soc.* **2009**, *131*, 11147.
[13] B. J. Schultz, C. J. Patridge, V. Lee, C. Jaye, P. S. Lysaght, C. Smith, J. Barnett, D. A. Fischer, D. Prendergast, S. Banerjee, *Nat. Commun.* **2011**, *2*, 372.
[14] L. Y. Jiao, L. Zhang, X. R. Wang, G. Diankov, H. J. Dai, *Nature* **2009**, *458*, 877.

[15] D. V. Kosynkin, A. L. Higginbotham, A. Sinitskii, J. R. Lomeda, A. Dimiev, B. K. Price, J. M. Tour, *Nature* **2009**, *458*, 872.
[16] J. L. Wang, L. Ma, Q. H. Yuan, L. Y. Zhu, F. Ding, *Angew. Chem.* **2011**, *123*, 8191; *Angew. Chem. Int. Ed.* **2011**, *50*, 8041.
[17] M. J. McAllister, J.-L. Li, D. H. Adamson, H. C. Schniepp, A. A. Abdala, J. Liu, M. Herrera-Alonso, D. L. Milius, R. Car, R. K. Prud'homme, I. A. Aksay, *Chem. Mater.* **2007**, *19*, 4396.
[18] X. F. Gao, L. Wang, Y. Ohtsuka, D.-E. Jiang, Y. L. Zhao, S. Nagase, Z. F. Chen, *J. Am. Chem. Soc.* **2009**, *131*, 9663.
[19] S. Fujii, T. Enoki, *J. Am. Chem. Soc.* **2010**, *132*, 10034.
[20] J.-L. Li, K. N. Kudin, M. J. McAllister, R. K. Prud'homme, I. A. Aksay, R. Car, *Phys. Rev. Lett.* **2006**, *96*, 176101.
[21] Z. Y. Li, W. H. Zhang, Y. Luo, J. L. Yang, J. G. Hou, *J. Am. Chem. Soc.* **2009**, *131*, 6320.
[22] J. Liu, A. G. Rinzler, H. J. Dai, J. H. Hafner, R. K. Bradley, P. J. Boul, A. Lu, T. Iverson, K. Shelimov, C. B. Huffman, F. Rodriguez-Macias, Y.-S. Shon, T. R. Lee, D. T. Colbert, R. E. Smalley, *Science* **1998**, *280*, 1253.
[23] G. Kresse, J. Hafner, *Phys. Rev. B* **1993**, *48*, 13115.
[24] G. Kresse, J. Furthmuller, *Comput. Mater. Sci.* **1996**, *6*, 15.
[25] J. P. Perdew, K. Burke, M. Ernzerhof, *Phys. Rev. Lett.* **1996**, *77*, 3865.
[26] P. E. Blöchl, *Phys. Rev. B* **1994**, *50*, 17953.
[27] G. Kresse, D. Joubert, *Phys. Rev. B* **1999**, *59*, 1758.
[28] G. Henkelman, B. P. Uberuaga, H. Jonsson, *J. Chem. Phys.* **2000**, *113*, 9901.
[29] R. P. Bell, *Proc. R. Soc. London Ser. A* **1936**, *154*, 414.
[30] M. G. Evans, M. Polanyi, *Trans. Faraday Soc.* **1938**, *34*, 11.
[31] S. P. Koenig, N. G. Boddeti, M. L. Dunn, J. S. Bunch, *Nat. Nanotechnol.* **2011**, *6*, 543.
[32] Z. H. Ni, T. Yu, Y. H. Lu, Y. Y. Wang, Y. P. Feng, Z. X. Shen, *ACS Nano* **2008**, *2*, 2301.
[33] T. M. G. Mohiuddin, A. Lombardo, R. R. Nair, A. Bonetti, G. Savini, R. Jalil, N. Bonini, D. M. Basko, C. Galiotis, N. Marzari, K. S. Novoselov, A. K. Geim, A. C. Ferrari, *Phys. Rev. B* **2009**, *79*, 205433.
[34] M. Y. Huang, H. G. Yan, C. Y. Chen, D. H. Song, T. F. Heinz, J. Hone, *Proc. Natl. Acad. Sci. USA* **2009**, *106*, 7304.
[35] L. Gong, I. A. Kinloch, R. J. Young, I. Riaz, R. Jalil, K. S. Novoselov, *Adv. Mater.* **2010**, *22*, 2694.
[36] M. Y. Huang, H. G. Yan, T. F. Heinz, J. Hone, *Nano Lett.* **2010**, *10*, 4074.
[37] R. J. Young, L. Gong, I. A. Kinloch, I. Riaz, R. Jalil, K. S. Novoselov, *ACS Nano* **2011**, *5*, 3079.

